Investigation of the doping profile of a non-intentionally doped epitaxial layer of a PIN photodiode

Raphael P. L. Steimvacher
Spatial Sensor and Actuators/CTE-S
Institute Of tecnological Aeronautics
São Jose dos Campos, Brazil
https://orcid.org/0000-0003-3368-1140

Cristian A. Delfino
subdivison of technologies for Infrared/EFA-I
Institute of Advanced Studies/IEAv
São Jose dos Campos, Brazil
cris.delfino@gmail.com

Gustavo S. Vieira
subdivison of technologies for Infrared/EFA-I
Institute of Advanced Studies/IEAv
São Jose dos Campos, Brazil
https://orcid.org/0000-0002-9512-0026

Rudy M. S. Kawabata
Semiconductor laboratory/CETUC
Pontifical Catholic University of Rio de janeiro
Rio de Janeiro, Brazil
rudykawa@gmail.com

Mauricio P. Pires
Physics Institute
Federal University of Rio de Janeiro
Rio de Janeiro, Brazil
pires@if.ufrj.br

Patricia L. de Souza
Semiconductor laboratory/CETUC
Pontifical Catholic University of Rio de janeiro
Rio de Janeiro, Brazil
https://orcid.org/0000-0001-8752-5958

***Abstract*— The non-intentionally doped epitaxially grown layer of a PIN photodiode is investigated using C-V measurements to obtain its doping profile. The non-intentionally doped layer of $In_{0.53}Ga_{0.47}As$, epitaxially grown, , on a n^+ layer of the same material showed values around ~10^{16} cm^{-3} close to its top and ~10^{17} cm^{-3} still above the lower ¼ of the layer, suggesting a significant doping segregation from the n^+ bottom layer.**

Keywords—Doping profile, segregation, epitaxial growth, C-V measurements

I. INTRODUCTION

The realization of atomically standardized and abrupt layers is a matter of great concern for the semiconductor field, but, though advances in Crystal growth techniques, such as molecular beam epitaxy (MBE) and metal-organic vapor phase epitaxy (MOVPE), have obtained high-quality films, some physical limitations, such as diffusion and segregation, have kept one from completely reaching this goal. In the MOVPE growth of III-V compound semiconductors, for example, it has been reported a considerable amount of Al atoms segregation to the surface of InGaAs/AlGaAs layers, other study related the segregation of Sb to surface of n InAs/$InAs_{1-x}Sb_x$ layers. This segregation of III-V compounds limits abrupt interface attainment. [1-6]

The growth of non-intentionally doped (NID) layers over heavily doped layers can also be affected by a segregation of dopants from heavily doped layer to NID layer, this migration of dopants can be described by an exponential decay as a function of position, as discussed in the literature, [7-12] although this NID layer may have some residual doping concentration even without any segregation. For example, InP and InGaAs NID layers are found to have n type residual doping concentrations of order of 10^{15} to 10^{16} cm^{-3}. [13-15] Dopant impurities can be transferred from the heavily doped base layer to the growing NID layer or be diffused from the also heavily doped top layer (although it is a smaller effect), impacting, for example, a PIN photodiode absorbing layer, that should be non-intentional doped (NID), reducing its quantum efficiency. [16]

There are several techniques for the investigation of doping profile in an epitaxial layer, among them: spreading resistance method (SRM), capacitance-voltage methods, secondary ion mass spectrometry (SIMS), neutron activation analysis (NAA), etc., whether they are destructive or non-destructive. [17] Here, the investigation of the doping profile of the NID layer of a PIN photodiode is done via a capacitance-voltage measurement (C-V) technique. This non-destructive technique allows obtaining the active impurities in the absorbing layer of the photodiodes using the theory of Hilibrand and Gold. [18, 19]

II. EXPERIMENTAL DETAILS

Lattice-matched $In_{0.53}Ga_{0.47}As$/InP PIN photodiodes were grown by metalorganic vapor phase epitaxy (MOVPE). The structure consists of a 200 nm top $In_{0.53}Ga_{0.47}As$ layer with a Zn doping density of $1.5 \times 10^{19} cm^{-3}$ (p-region) followed by a 2.0 µm NID (non-intentionally doped) $In_{0.53}Ga_{0.47}As$ absorption layer (I-region) on a 600 nm $In_{0.53}Ga_{0.47}As$ layer with a Si doping density of 2×10^{18} cm^{-3} (n-region) over a semi insulating (Fe doped) InP substrate.

A schematic picture of the structure can be seen in Fig 1. The devices were processed into mesa structure, using standards photolithography techniques with wet etching, where all devices are on the same substrate and share the same epitaxically grown layers, being replicas of the same photodiode.

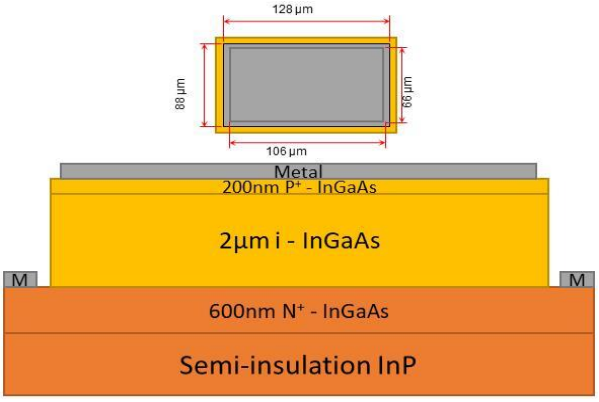

Fig. 1. Schematic of the PIN photodiode mesa structure.

For the characterization, a B1500 parameter analyzer from Keysight was used and the contacts in the sample were performed using a probe-station CCR10-2 (4TX-2) from Janis Research CO. Inc. The polarization was done taking the bottom contact as ground, ramping the reverse voltage from 0V to 25V and decreasing reverse bias from 25V to 0V, in C-V measurements. This bias range was enough to probe near half of the nominal absorber layer width.

III. Results and Discussion

A typical C-V data measured is shown in fig. 2. From this data the doping profile of the absorbing layer can be obtained. [18]

According to the basic literature, the junction capacitance decreases with the inverse of square root of reverse bias, when the layers are uniformly doped, and the depletion region is mainly in the less doped side, when one side is much more doped than the other. [20] In the present work, the p^+ layer is much more doped than the NID layer, each has a *n* type residual doping. To calculate the variation of the depletion region width (W), we use equation 1, which is valid even for the non-uniformly doped case. [21]

$$W = \frac{\varepsilon_r \varepsilon_0 A}{C}; \quad (1)$$

where, ε_r is relative permittivity of the material, ε_0 is permittivity of vacuum, A is area of device and C is the differential capacitance.

For computing the depletion region width, three curves of the inverse of square root of reverse bias were fitted to the data, each one covering a region of the graph in fig. 2, the first fit from 0 V to 3 V range, the second fit from 2 V to 11 V range, and the third fit from 10 V to 25 V range, in order to smooth the noise seen in the capacitance data, then depletion region is estimated using the first fit from the range 0 V to 2.10 V, the second fit from the range 2.13 V to 10.08 V, and the third fit from the range 10.11 V to 25 V (there is an intersection between adjacent fitting ranges, to avoid fitting border effects). The graph of depletion as a function of the reverse voltage is shown in fig. 3.

If the plot of the fig. 3 followed a square root dependency (uniformly doped layer), the plot of the inverse of the square of the capacitance (proportional to the square of the depletion width) would be a straight line. Such plot is shown in fig. 4, presenting a clearly non-linear curve.

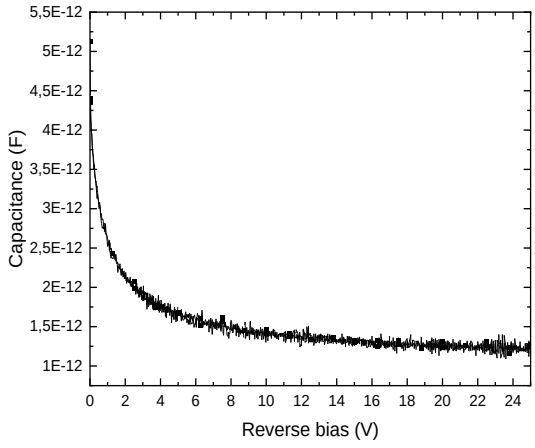

Fig. 2. A typical C-V data from one of the PIN photodiodes.

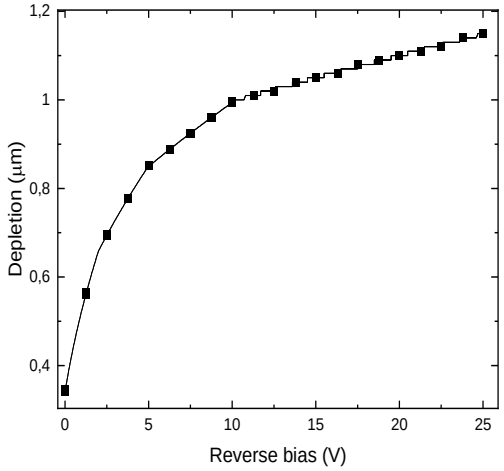

Fig. 3. Graph of the depletion width as a function of the reverse voltage of one of the PIN photodiodes.

From the graph in fig. 4, the doping level at the depletion region limit in the light doped layer can be obtained, using equation 2. [17, 20]

$$N = \frac{2}{q\varepsilon_r \varepsilon_0 A^2} \frac{1}{\frac{d(\frac{1}{C^2})}{dVr}}; \quad (2)$$

where N is the doping concentration, q is elementary charge, ε_r the relative permittivity of the material, ε_0 is permittivity of vacuum, A the sample area, C is the differential capacitance and V_r is the reverse bias.

The derivative of the curve in fig. 4, which is needed in equation 2, was obtained making 3 quadratic fits distributed by region on the curve, the first fit from 0 V to 7 V range, the second fit from 3 V to 12 V range, and the third fit from 6.5 V to 25 V range. It was needed because a single fit would not fit well the whole curve. After performing these quadratic fits and obtained the corresponding equations, the derivate was calculated for the first fit and used in equation 2 to obtain the doping concentration in the range 0 V to 5.08 V, the derivate of second fit was used in range of 5.10 V to 9.50 V, and the derivate of third fit was used in range of 9.53 V to 25 V (there is an intersection between adjacent fitting ranges, to avoid fitting border effects).

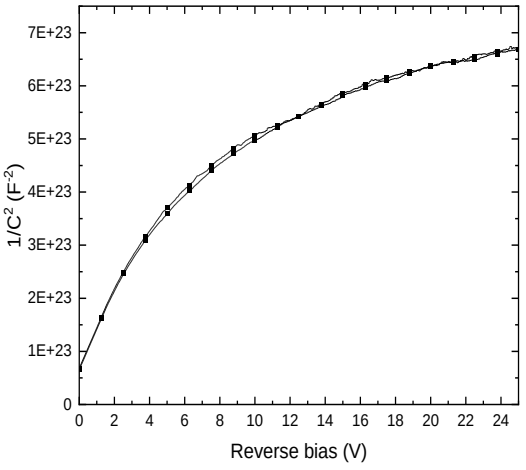

Fig. 4. Graph of the inverse of the square of capacitance as a function of reverse voltage of one of the PIN photodiodes.

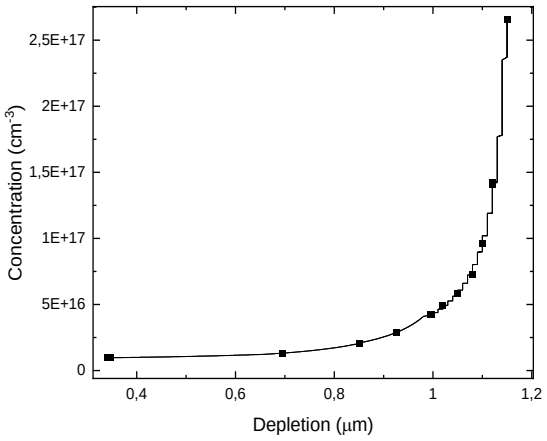

Fig. 5. Graph of the doping profile of the NID layer of one of the PIN photodiodes.

The doping concentration obtained, for one of the devices, as a function of depletion layer width, is plotted on fig. 5. It is the doping concentration at a depletion region width from the topo of the NID layer.

In fig. 5, a n type doping concentration ranging from a value close to the expected for the residual doping of a NID layer, to a value near one order of magnitude higher can be seen. It was not possible to reach the bottom of the NID layer (2 μm) due avalanche current. The increase in doping concentration from the top to the bottom of the NID layer suggests a significant doping segregation. In fig. 6, it is shown that the behavior is similar when other devices on the same sample piece (same substrate, same epitaxial layers and same microfabrication process) are measured, as expected.

As seen in figs. 5 and 6, the increase on doping concentration suggests a doping segregation coming from the bottom heavily doped layer to the NID layer. A way of expressing the segregation is by a segregation length, which can be obtained by an exponential fit to the curves, obtaining segregation coefficients of 1.12 ± 0,03 nm for device 1, 1.20 ± 0,02 nm for device 2 and 1.14 ± 0,02 nm for device 3. Compared to other segregation lengths obtained in the literature they are in the same order of magnitude, ranging from 2.4 nm to 5 nm. [7, 10]

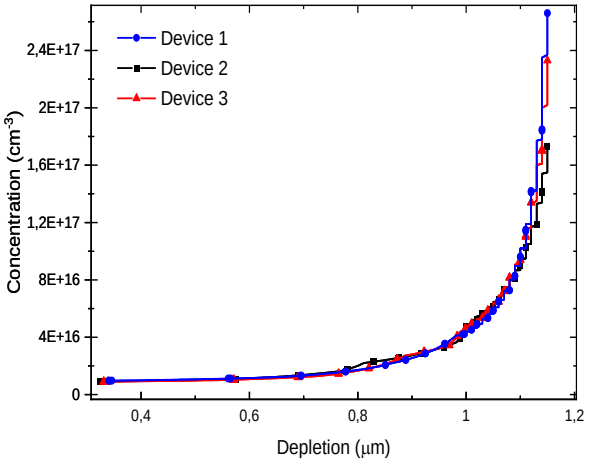

Fig. 6. Graph of doping profile of the NID layer of 3 photodiodes on the same sample.

Although a diffusion length of the same order of magnitude of the ones reported in the literature were found, the fit of a *S* curve (equação 3) gives doping concentration to the bottom n^+ layer significantly larger than the nominal of 2 x 10^{18} cm^{-3}. It needs to be futher investigated, other dopping mechanisms mignt be taking effect, giving an effective doping profile that follows a different function.

$$S = yo + \frac{N_{n+}}{1+e^{-k(x-xo)}}; \quad (2)$$

where N_{n+} is the doping concentration to the bottom n^+ layer, yo is residual doping, k is the inverse of segregation coefficient, xo is the interface point between NID layer and the bottom layer N^+.

CONCLUSION

The Investigation of the doping profile of a non-intentionally doped layer of $In_{0.53}Ga_{0.47}As$, epitaxially grown on a n^+ layer of the same material was obtained using C-V measurements. The data showed an increasing concentration from top to down ranging from ~10^{16} cm^{-3}, close to the top of the NID layer, to ~10^{17} cm^{-3} at a depth of ~1.1 μm. Since the NID layer is expected to have a width of 2 μm, the data suggests a doping segregation from the n^+ bottom layer, with segregation length in the range of 1.12 nm to 1.20 nm, at the same order of magnitude presented in the literature (2.4 nm to 5 nm). The doping concentration obtained close to the top of the NID layer showed a value around what can be expected for the residual doping of such layer, according to what was found in the literature (10^{15} to 10^{16} cm^{-3}). [13-15]

ACKNOWLEDGMENT

The authors are grateful to Institute for advanced Studies (IEAV) for the use of the LCDS laboratory and to the financial support of FINEP, CNPq and FAPERJ. This study was financed in part by the Coordenação de Aperfeiçoamento de Pessoal de Nível Superior - Brasil (CAPES) - Finance Code 001.

REFERENCES

[1] K. Muraki, S. Fukatsu, Y. Shiraki, R. Ito. “Surface segregation of In atoms during molecular beam epitaxy and its influence on the energy levels in InGaAs/GaAs quantum wells”. Appl. Phys. Lett., v. 61, n. 5, p. 557-468, 3 August 1992. https://doi.org/10.1063/1.107835.

[2] J. M. Moison, C. Guille, F. Houzay, F. Barthe, M. Van Rompay. “Surface segregation of third-column atoms in group III-V arsenide compounds: Ternary alloys and heterostructures”. Phys. Rev., v. 40, n. 9, p. 9-15, 15 September 1989. https://doi.org/10.1103/PhysRevB.40.6149.

[3] C. Frigeri, A. Di Paola, N. Gambacorti, D.M. Ritchie, F. Longo, M. Della Giovanna. “Transmission electron microscopy and X-ray diffraction investigation of In segregation in MOVPE-grown InGaAs-based MQWs with either GaAs or AlGaAs barriers”. Materials Science and Engineering: B. v. 28, n. 1–3, p. 346-352, December 1994. https://doi.org/10.1016/0921-5107(94)90080-9.

[4] Xiaodong Hao, Lei Li, Qingbo Kong, Shufang Ma, Jiahui Wang, Yang Xu, Xingyu Liu, Bin Han, Bocang Qiu, Bingshe Xu,. “Atomic-scale insights of the effect of growth temperature on the migration behavior of Al atoms in InGaAs/AlGaAs multiple quantum wells”. *Materials Science in Semiconductor Processing*, v. 154, 107197, February 2023. https://doi.org/10.1016/j.mssp.2022.107197.

[5] M. Choubani, H. Maaref, F. Saidi. “Indium segregation and In–Ga inter-diffusion effects on the photoluminescence measurements and nonlinear optical properties in lens-shaped InxGa1-xAs/GaAs quantum dots”. *Journal of Physics and Chemistry of Solids*, v. 160, 110360 January 2022. https://doi.org/10.1016/j.jpcs.2021.110360.

[6] Qun Yang, Renliang Yuan, Lingling Wang, Ruikai Shi, Jian-Min Zuo. “Antimony segregation in an InAs/InAs1−xSbx superlattice

grown by metalorganic chemical vapor deposition". *Journal of Applied Physics*. v. 130, 095302 7 September 2021. https://doi.org/10.1063/5.0060777.

[7] D. M. Pedroso, T. G. Santos, C. A. Delfino, G. S. Vieira, F. M. Fernandes, A. A. Quivy, A. Passaro. "Effect of dopant segregation and negative differential mobility on multi-quantum well activation energy". *J Mater Sci*. v. 52, 5223–5231, 13 Jnauary 2017. https://doi.org/10.1007/s10853-017-0763-9.

[8] C. B. Arnold, M. J. Aziz. "Unified kinetic model of dopant segregation during vapor-phase growth". *Physics Review B.* v.72, 195419, 18 November 2005. https://doi.org/10.1103/PhysRevB.72.195419.

[9] H. C. Liu, Z. R. Wasilewski, M. Buchanan, Hanyou Chu. "Segregation of Si δ doping in GaAs - AlGaAs quantum wells and the cause of the asymmetry in the current - voltage characteristics of intersubband infrared detectors". *Appl. Phys. Lett*. V. 63, n. 6, p. 761-763, 9 August 1993. https://doi.org/10.1063/1.109900.

[10] Z. R. Wasilewski, H. C. Liu, M. Buchanan. "Studies of Si segregation in GaAs using current–voltage characteristics of quantum well infrared photodetectors". *Journal of Vacuum Science & Technology B: Microelectronics and Nanometer Structures Processing, Measurement, and Phenomena*. V. 12, n. 2, p. 1273-1276, 1 March 1994. https://doi.org/10.1116/1.587020.

[11] J.J. Harris, J.B. Clegg, R.B. Beall, J. Castagné, K. Woodbridge, C. Roberts. "Delta-doping of GaAs and Al0.33Ga0.67As with Sn, Si and Be: a comparative study". *Journal of Crystal Growth*. v. 111, n.1-4, p. 239-245, 2 May 1991. https://doi.org/10.1016/0022-0248(91)90978-E.

[12] K. Muraki, S. Fukatsu, Y. Shiraki, R. Ito. "Surface segregation of In atoms during molecular beam epitaxy and its influence on the energy levels in InGaAs/GaAs quantum wells". *Appl. Phys. Lett.* v. 61, n. 5, p. 557-559, 3 August 1992. https://doi.org/10.1063/1.107835.

[13] M. Glade, J. Hergeth, D. Grützmacher, K. Masseli, P. Balk. "Diffusion of Zn acceptors during MOVPE of InP". *Journal of Crystal Growth*, v. 108, n. 3–4, p. 449-454, 1 february 1991. https://doi.org/10.1016/0022-0248(91)90221-P.

[14] Robert Chow, Young G. Chai. "Electrical and optical properties of InP grown by molecular beam epitaxy using cracked phosphine". *Appl. Phys. Lett*., V. 42, n. 4, p. 383-385, 15 February 1983. https://doi.org/10.1063/1.93947

[15] Thomas Kaltsounis, Helge Haas, Matthieu Lafossas, Simona Torrengo, Vishwajeet Maurya, Julien Buckley, Denis Mariolle, Marc Veillerot, Alain Gueugnot, Laurent Mendizabal, Yvon Cordier, Matthew Charles. "Characterization of unintentional doping in localized epitaxial GaN layers on Si wafers by scanning spreading resistance microscopy". *Microelectronic Engineering*. v. 273 , 111964, March 2023. https://doi.org/10.1016/j.mee.2023.111964.

[16] B. G. Streetman, S. K. Banerjee. *Solid state eletronic devices*. Seventh edition. Essex, England: Publised by Person Education Limited, 2016. p. 437-439.

[17] P. Gaworzewski, L. Kalman, H. Rausch, M. Trapp. "Doping profile techniques for Si epitaxial layers". *J. Radioanal. Chem.* v. 52, n. 1, p. 93-100, March 1979. https://doi.org/10.1007/BF02517703

[18] Cristea, Miron J. "Capacitance-voltage Profiling Techniques for Characterization of Semiconductor Materials and Devices". *Electronics & Instrumentation Engineering: An international Journal (EEIEJ)*, v. 1, n. 3, August 2014. http://dx.doi.org/10.2139/ssrn.3433675

[19] D. Salameh and D. Linton D. "Study of the relation between doping profile and diode CV characteristics," *in IEEE Transactions on Microwave Theory and Techniques*, v. 47, n. 4, p. 506-509, April 1999. doi: 10.1109/22.754885

[20] B. G. Streetman, S. K. Banerjee. *Solid state eletronic devices*. Seventh edition. Essex, England: Publised by Person Education Limited, 2016. p. 236-240.

[21] S. M. Sze, Kwok K Ng. *Physics of semiconductor devices*. Third edition. Hoboken, New jersey. Publised by john wiley & Sons, Inc. 2007. p. 86-90.